Journal of the Korean Society of Propulsion Engineers
Vol. 23, No. 1, pp. 61-70, 2019

Research Paper
DOI: http://dx.doi.org/10.6108/KSPE.2019.23.1.061

플라즈마 풍동의 초음속 마하 디스크 특성

Rajesh Kumar Chinnaraj[a] · 오필용[b] · 최성만[a,*]

Supersonic Mach Disk Characteristics in a Plasma Wind Tunnel

Rajesh Kumar Chinnaraj[a] · Philyong Oh[b] · Seongman Choi[a,*]
[a] *Aerospace Engineering Department, Chonbuk National University, Korea*
[b] *High Enthalpy Plasma Research Center, Chonbuk National University, Korea*
[*] *Corresponding author. E-mail: csman@jbnu.ac.kr*

ABSTRACT

A primary investigation on the underexpanded flow generated in a 0.4 MW class high enthalpy supersonic arc-heated plasma wind tunnel is conducted experimentally. The diameter and the position of the Mach disk from the nozzle exit is measured for overall pressure ratios ranging from 200 to 30. The empirical correlations for Mach disk diameter and position are determined which show very good agreement with experimental results.

초 록

0.4 MW 급 고 엔탈피 초음속 아크 가열 플라즈마 풍동에서 발생된 팽창 유동에 대한 기초연구를 실험적으로 완료하였다. 노즐 출구로부터의 마하 디스크의 직경과 위치는 전체 압력비가 200에서 30까지 측정되었다. 마하 디스크 직경과 위치에 대한 경험적인 상관관계는 실험결과와 매우 일치하는 결과를 얻었다.

Key Words: Underexpanded flow(과소팽창유동), Mach disk(마하 디스크), Overall pressure ratio (전 압력비), Plasma wind tunnel(플라즈마 풍동)

1. Introduction

Plasma wind tunnels are extensively used for characterization and validation of the materials suitable for thermal protection systems (TPS) for spacecrafts. TPS are single points of failure for spacecrafts involving in atmospheric entry or re-entry which include manned, sample return and interplanetary rover landing missions. Spacecrafts encounter high thermal and high velocity ablative plasma

Received 18 June 2018 / Revised 29 November 2018 / Accepted 1 December 2018

pISSN 1226-6027 / eISSN 2288-4548
[이 논문은 한국추진공학회 2018년도 춘계학술대회(2018. 5. 30- 6. 1, 라마다프라자 제주호텔) 발표논문을 심사하여 수정・보완한 것임.]

flows due to combined effects of atmospheric drag and aerodynamic heating. It is utmost importance to test and validate the behaviour of TPS-candidate materials in the test flows which stimulate the extreme conditions expected during atmospheric entry or re-entry regime.

Plasma wind tunnel facility at Chonbuk National University's High Enthalpy Plasma Research Center is designed and equipped for rigorous characterization and validation of TPS-candidate materials[1, 2]. This facility houses a high enthalpy supersonic arc-heated plasma wind tunnel of 0.4 MW class (hereafter PWT) capable of stimulating ablative conditions encountered during atmospheric re-entries.

One of the prerequisites for proper optimization of PWT is to understand the plasma test flow generated in the plasma wind tunnel. In other words, the high efficient validation of TPS-candidate materials by using the PWT depends on the effective characterisation of the plasma test flow. In order to operate and generate high enthalpy supersonic plasma flow in the PWT, a very high pressure is maintained in plasma generating torch and a very low pressure is maintained in test chamber. The torch acts as a high pressure reservoir while the test chamber acts as a low pressure ambience. When the generated plasma flow extrudes from plasma generating section of the torch into the test chamber through a convergent-divergent nozzle, by nature the resultant flow obtained in test chamber is supersonic underexpanded flow. Based on the structure, underexpanded flow can be categorized into i) very highly underexpanded jet ii) highly underexpanded jet and iii) moderately underexpanded jet. This depends on the overall pressure ratio ($P_{reservoir}/P_{ambient}$), a very high difference between reservior and ambient pressure results in a highly underexpanded flow, while low overall pressure ratios result in moderately underexpanded flows. Generally, in case of very highly and highly underexpanded jets, as the flow exits the nozzle into very low pressure ambience, expansion waves are formed and expand upto jet boundary where they get reflected towards axis of the jet in form of weak compression waves. These compression waves then merge into an oblique shock called as intercepting shock. The Mach disk, a shock normal to the jet axis is formed. The intercepting shock interacts with Mach disk and reflected into an another oblique shock. The Mach number profile of the flow across the shocks[3, 4] is shown in Fig. 1.

It is important to note that Mach disk is not formed in the moderately underexpanded flows which are characterized by formation of diamond shape structures. (For more clarity, refer Figs. 7, 8 and 9 in section 3.)

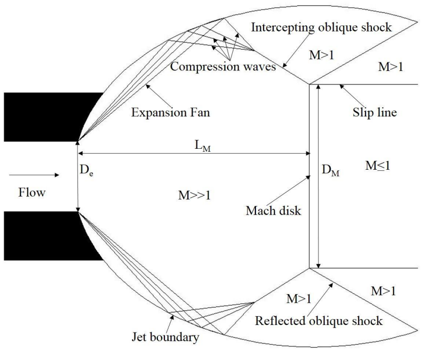

Fig. 1 Schematics of Mach disk formation.

Table 1. Underexpanded flow categories.

Case	Mach disk	Secondary shock cells
i. Moderately	No	Yes
ii. High	Yes	Yes
iii. Very high	Yes	No

Even though underexpanded flows are comprehensively studies in researches related aircraft and rockets exhaust plumes and also in fields involving accidental leakage of highly pressurized gases, the studies of underexpanded flow in a plasma wind tunnel with respect to material testing are limited. The broad knowledge of underexpanded flow in the PWT is vital for better characterization of TPS-candidate material, especially the location of Mach disk. As the nature of flow changes abruptly from supersonic to subsonic across the Mach disk, the Mach disk characterization will help in determining better exposure location for material specimen in the plasma test flow. The aim of this study is to measure the position and the diameter of the Mach disk with respect to variations in η_o, where η_o is the overall pressure ratio of the convergent-divergent nozzle. In case of the PWT, η_o is the ratio of the pressure in plasma generating torch to the test chamber pressure. The another main purpose of this study is to understand the aerodynamics of high temperature plasma flow. Apart from testing the materials related to space applications, there are some fascinating future applications for plasma in field of aerospace[5-7]. The aerodynamic applications of plasma include plasma-based flow control and plasma-assisted ignition and combustion technology. Plasma has been found very useful to control boundary layer and flow separation, to initiate combustion and stabilize flame in the combustion chamber. Adamovich et al.[8] have discussed effects of plasma in shock wave propagation. The four effects discussed in their work are 1. shock acceleration, 2. nonmonotonic variation of flow parameters behind the shock front, 3. shock weakening, and 4. shock splitting and spreading. They have discussed various reasons for these effects to occur and emphasized the need for more experiments to understand the plasma shock phenomena. The experimental works of Merriman et al.[9] and Palm et al.[10] of Ohio state university have proved that shock weakening effect observed in supersonic plasma flow is mainly due to thermal effects caused by interaction between heated boundary layer and shock wave and is not solely due to plasma effects. The above mentioned research works are focused on weakly ionized non equilibrium plasma (cold plasma).

The research works related to shockwaves in underexpanded high temperature plasma flows with strong ionization are very limited. The thermal non-equilibrium characteristics of plasma also defines how plasma behave aerodynamically. But throughout literature, many researches have assumed plasma to be in locally thermodynamic equilibrium (LTE) conditions to derive thermodynamic properties of the plasma[11-13]. A similar approach has been adopted in this study to obtain thermodynamic properties of the generated plasma flow. The boundary layer formed by the plasma flow on the nozzle wall is not only an aerodynamic problem but also should treated as a surface electro-chemistry problem. The effects of Debye sheath[14] and effects of free electrons on the heat transfer across the plasma-nozzle wall boundary layer[15] are some of the characteristics which are unique only to plasma flow and have to be carefully considered while investigating the aerodynamics properties of the plasma flow. In this experimental research work, the diameter and position of Mach disk formed in high enthalpy plasma flow is measured and compared with other similar previously conducted research works. This help us to understand plasma-aerodynamics of flow generated in a high enthalpy supersonic arc-heated plasma wind tunnel.

2. Experimental Details

2.1 0.4 MW Class Arc Heated Plasma Wind Tunnel

The components of the 0.4 megawatt class supersonic plasma wind tunnel include gas supply manifold, segmented type arc plasma torch, test chamber, diffuser, heat exchanger, cooling water supply, DC power supply and vacuum pump system.

During the operation, the test chamber of the plasma wind tunnel is sealed and depressurized by using the vacuum pump system. On reaching a desired low pressure condition in the test chamber, a very small percentage of argon passed between anode and cathode of the plasma arc torch. When the power is applied, the very high potential difference between the electrodes causes an electric arc to be struck between them along the initial stream of argon. Then a mixture of air and argon called as carrier or working gas is fed through the individual segments of the plasma torch. The working gas interacts with

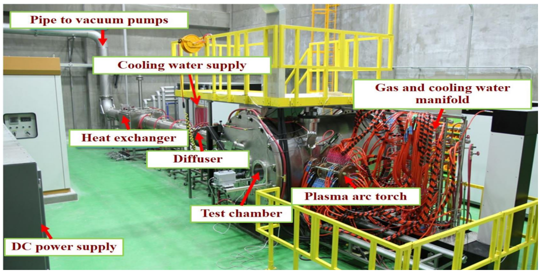

Fig. 2 0.4 MW class arc heated plasma wind tunnel.

Table 2. Plasma flow properties.

Plasma flow property	Values
Total specific enthalpy(MJ/kg)	11.471
Temperature(K)	4985.4
Density(kg/m^3)	2.583×10^{-3}
Specific heats ratio (γ)	1.132
Nozzle exit Mach number	2.11

the electric arc which leads to dissociation and ionization of gas molecules. The generated high temperature plasma is then passed through a convergent-divergent nozzle resulting in a supersonic flow. The test chamber is connected to a diffuser and a heat exchanger which decelerate and cool down the high temperature supersonic flow respectively once it exist the test chamber.

2.2 Test Condition

To generate plasma test flow, a total inlet gas mass flow rate of 12.17 g/s (95% air and 5% argon) was fed into the arc-jet plasma generating torch.

For this experiment a plasma torch nozzle with a throat diameter of 10.6 mm and a exit diameter of 16 mm was used. A total average power of 295.76 kW was applied between the electrodes of the segmented arc-jet plasma torch. Applying the energy balance method[16] on the plasma generating torch and using NASA's CEA codes[17-21], following plasma flow parameters were estimated. The plasma flow generation was initiated at a η_o < 2000, as the flow extruded into test chamber η_o decreased quickly. The Mach disk started to appear clearly in field of visibility (limited by dimensions of the visual ports on the test chamber) around η_o = 200.

The above Figs 3, 4, 5 and 6 show the operating conditions of the PWT during the experiment. The highlighted region 2 represents conditions where the Mach disk is clearly visible through visual ports of the test chamber. The region 3 represents the conditions related moderately underexpanded flow (absence of Mach disk). Hence the position and diameter of the Mach disk are measured only for the conditions in the region

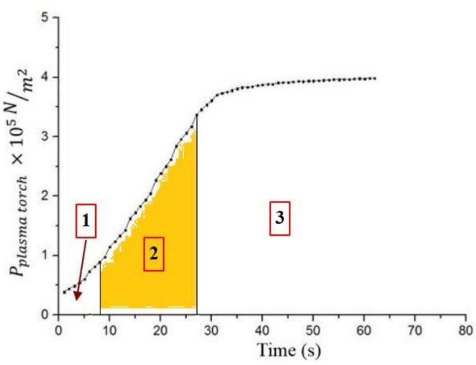

2 .

Fig. 3 Plasma torch pressure versus time.

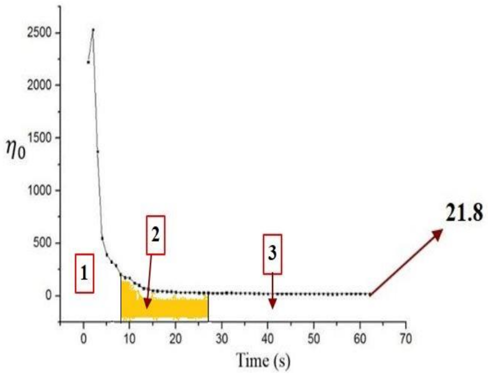

Fig. 5 Overall pressure ratio (η_o) versus time.

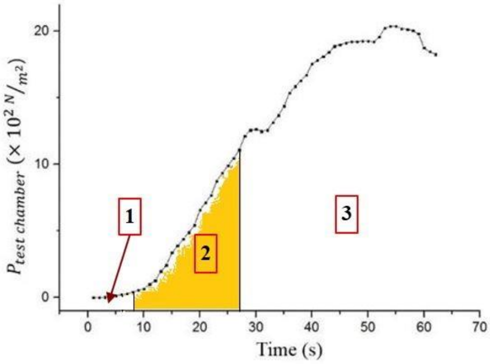

Fig. 4 Test chamber pressure versus time.

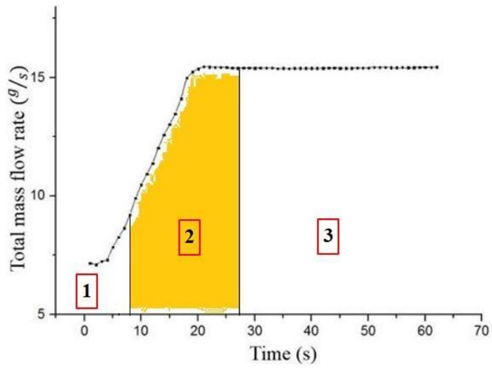

Fig. 6 Total mass flow rate versus time.

The Mach disk formation is clearly visible to the naked eye and there is no need for special technique or method to visualize, capture and measure the diameter and length of the Mach disk which can be conveniently done using the photographs of the plasma flow and corresponding pressure conditions. The PWT operating conditions like test chamber pressure, plasma generating torch pressure and gas mass flow rates are measured using the sensors inside PWT. These data are recorded by PWT's console computer which helps to operate and monitor PWT. The generated plasma is recorded using a camcorder mounted on the side optical access window of PWT. By synchronizing time stamps of camcorder with PWT console computer, the pictures are compared with corresponding pressure data values. Using these pictures or frames the Mach disk position and diameter is measured using a drafting software with respect to the nozzle position and the values are non-dimensionalised using nozzle diameter.

3. Results and Discussion

The photographs of very highly, highly and moderately underexpanded flow obtained during the experiment are shown as Fig. 7, 8 and 9.

At η_o<30, the nature of the flow develops

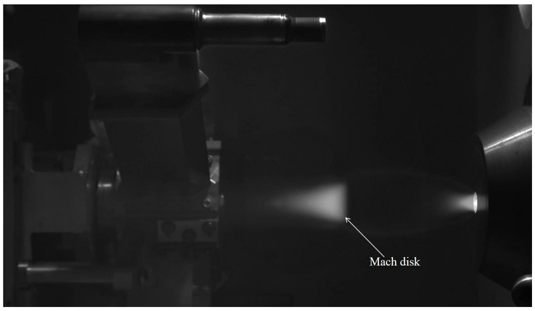

Fig. 7 Case 1 data (η_o $\approx$ 170).

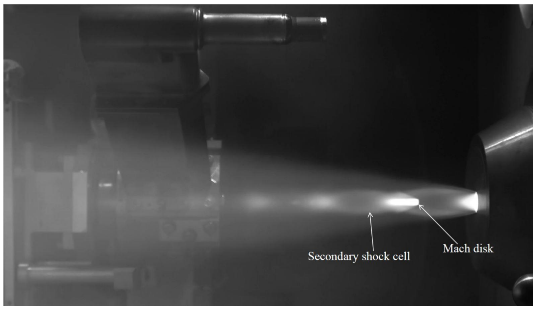

Fig. 8 Case 2 data (η_o $\approx$ 30).

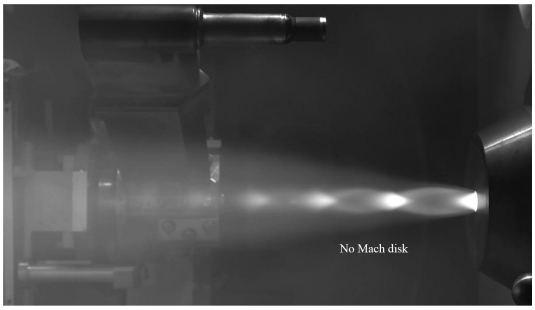

Fig. 9 Case 3 data (η_o< 30).

into a moderately undexpanded flow instantly with disappearance of Mach disk and appearance of diamond shaped structures. The variation in the structure of the flow temporally is shown as Fig. 10. In Fig. 10, transition of flow from very highly underexpanded flow to moderately underexpanded flow is clearly visible.

The Mach disk position (L_M) from the nozzle exit is non-dimensionalized using

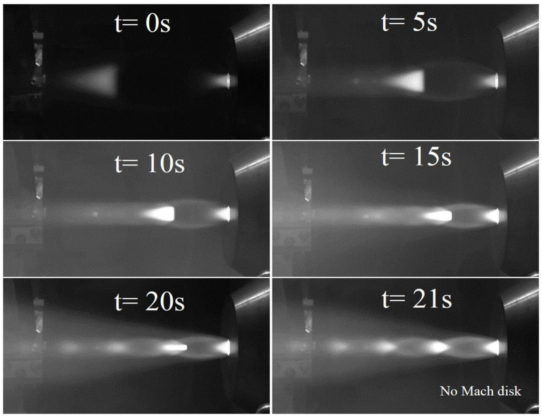

Fig. 10 Underexpanded flow transition.

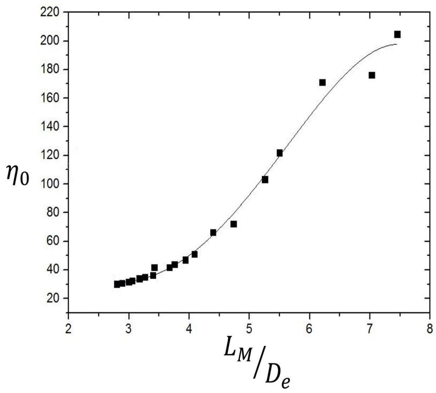

Fig. 11 Mach disk position vs η_o.

nozzle exit diameter (D_e) and it's variation with η_o is shown as Fig. 11.

The position of the Mach disk moves away from the nozzle exit as the η_o increases. From the experimental data, following empirical correlation has been derived.

$$\frac{L_m}{D_e} = 0.534347\sqrt{\eta_0} \tag{1}$$

The above experimental results agrees well with the results of Crist et al.[3], who have developed a similar empirical correlation for their data as below.

$$\frac{L_m}{D_e} = 0.645497\sqrt{\eta_0} \quad (2)$$

Crist et al. used a hot-shot wind tunnel facility for stagnation temperature ranges from 300 K to 4200 K. Their empirical correlation is based on data obtained for their entire temperature range (300 K-4200 K), while the empirical correlation (Eq. 1) obtained in this study corresponds to the thermodynamic properties given in Table 2.

The correspondence between $\frac{L_M}{D_e}$ ratios measured from experimental data and $\frac{L_M}{D_e}$ ratios calculated from the empirical correlation (Eq. 1) shown as Fig. 11. From the Fig. 12, it is very clear that the empirical correlation obtained for $\frac{L_M}{D_e}$ is in good agreement with experimental results.

Relationship between the Mach disk diameter and η_o is presented as Fig. 13.

Fig. 13 also trends similarly to Fig. 11, the diameter of the Mach disk (D_M) increases with η_o. The corresponding empirical correlation is derived as below.

$$\frac{D_M}{D_e} = 2.224\log\eta_0 - 3 \quad (3)$$

$\frac{D_M}{D_e}$ ratios calculated from above the correlation are plotted along with $\frac{D_M}{D_e}$ ratios measured from the experiment and shown in Fig. 14. The Fig. 14 reveals that empirical

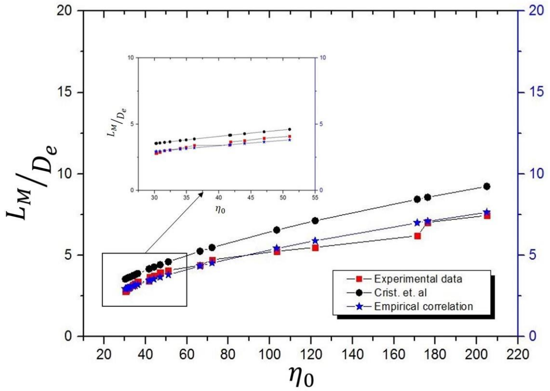

Fig. 12 Correspondence between experimental data and empirical correlation (Eq. 1).

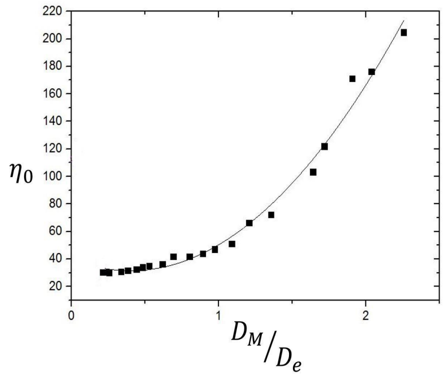

Fig. 13 Mach disk diameter vs η_o.

correlation for $\frac{D_M}{D_e}$ imitates the experimental results with a considerable accuracy. The above results also corresponds fairly with a similar empirical correlation found in research work of Antsupov[22] for cold air jets. Antsupov's empirical correlation for $\frac{D_M}{D_e}$ has been modified in terms of overall pressure ratio (η_o) and can be written as,

$$\frac{D_M}{D_e} = 2.5\log[\eta_0 \times (1+\frac{\gamma-1}{2}M^2)^{-(\frac{\gamma}{\gamma-1})}] - \frac{3}{4} \quad (4)$$

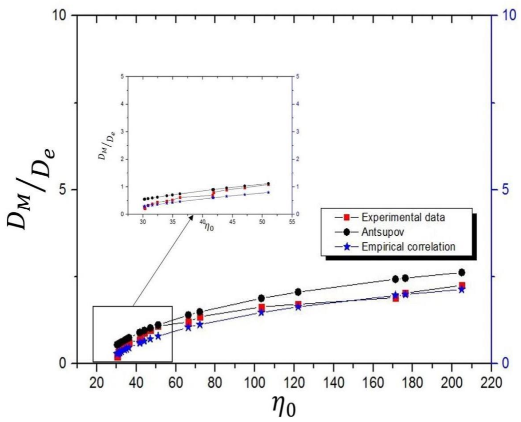

Fig. 14 Correspondence between experimental data and empirical correlation (Eq. 3).

Based on observation and experimental results, it is evident that overall pressure ratio is one of the critical factors influencing the diameter and position of the Mach disk in the underexpanded flow. The comparison of results with the previous research work conducted in general cases reveal the Mach disk position and diameter follow a similar tread with respect to overall pressure ratio. A decrease in Mach disk position and diameter has been observed in the current results. The reasons for this observed phenomenon maybe 1) shock weakening by plasma properties. 2) Thermal effects caused by high temperature nature of flow. Although an earlier research work[10] have observed that shock weakening in plasma flow only due to thermal effect, but the flow they have considered is weakly ionized cold plasma, where as the flow generated in this study is considered to be strongly ionized because of high enthalpy and arc-generated. The strong ionization effects on the Mach disk formation has to be considered. More exclusive studies needed to be done for determining thermal and ionization effects on the Mack disk formation in high enthalpy plasma flow. This will lead to better understanding of Mach disk and underexpanded test flows for more accurate TPS material testing and evaluation which is the main purpose of this PWT. Also more experimental work has to be accomplished to determine dependency of Mach disk diameter and position on other factors like specific heats ratio, nozzle geometry, flow rate and input power of PWT.

4. Conclusions

Experiment to measure the positions and diameter of Mach disk in high enthalpy arc-heated plasma flow is described. The results also show that the nature of underexpanded flow extensively depends on the overall pressure ratio. The empirical correlations for determining Mach disk diameter and position are given as a function of overall pressure ratio which will help to determine better testing position during TPS-material evaluation experiments. Even though variation of Mach disk position and diameter trend similarly with previous studies, there is decrease in Mach disk position and diameter which may be due to thermal and strong ionization effects of the high enthalpy plasma flow.

Acknowledgements

This study was supported by a National Research Foundation (NRF) of Korea under contract 2017M1A3A3A03016311. This study was also supported by the Space Core Technology Development Program through the National Research Foundation of Korea funded by the Ministry of Science and ICT

(NRF-2014M1A3A3A02034622) and supported by research facilities in the Plasma Application Institute of Chonbuk National University. The contributions of the members of the High-Enthalpy Plasma Research Center to the construction and commissioning of the plasma wind tunnel are gratefully acknowledged.

References

1. Rajesh Kumar, C., Oh, P.Y. and Choi, S.M., et al., “An Experimental Setup for Analysis and Validation of Materials for Thermal Protection Systems using Plasma Wind Tunnel“, *Proceedings of the 8th Asian Joint Conference on Propulsion and Power*, AJCPP2016-040, Takamatsu, Japan, 2016.
2. Rajesh Kumar, C., Oh, P.Y. and Choi, S.M., “Enthalpy Estimation in a 0.4 MW Class Arc-Jet Plasma Wind Tunnel”, *Proceedings of the 9h Asian Joint Conference on Propulsion and Power*, AJCPP2018-062, Xiamen, China, 2018.
3. Crist, S., Sherman, P.M. and Glass, D.R., “Study of the Highly Underexpanded Sonic Jet”, *AIAA Journal*, Vol. 4, No. 1, pp. 68–71, 1966.4.
4. Franquet, E., Perrier, V., et. al., “Free Under Expanded Jets in a Quiescent Medium: A Review”, *Progress in Aerospace Sciences*, Vol. 77, pp. 25-53, 2015.
5. Poggie, J., McLaughlin T. and Leonov, S., “Plasma Aerodynamics: Current Status and Future Directions“, *AerospaceLab Journal*, Issue. 10, pp. 1-6, 2015.
6. Mulder, M., *Aeronautics and Astronautics,* Intechopen, 2011.
7. Rayle, W, “Plasma Propulsion Possibilities“, *IRE Transactions on Military Electronics*, Vol. MIL-3, Issue. 2, pp. 42-45, 1959.
8. Adamovich, I.V., Subramaniam, V.V., and Rich, J.W., “Phenomenological Analysis of Shock-Wave Propagation in Weakly Ionized Plasmas", *AIAA Journal,* Vol. 36, No. 5, pp. 816-822, 1998.
9. Merriman S., Ploenjes, E., et. al., “Shock Wave Control by Nonequilibrium Plasmas in Cold Supersonic Gas Flow”, *AIAA Journal*, Vol. 39, No. 8, pp. 1547-1552, 2001.
10. Palm, P., Meyer, R., et al., "Nonequilibrium Radio Frequency Discharge Plasma Effect on Conical Shock Wave: M = 2.5 Flow", *AIAA Journal*, Vol. 41, No. 3, pp. 465-469, 2003.
11. Capitelli, M., Colonna, G., Gorse, C., et al., “Transport Properties of High Temperature Air in Local Thermodynamic Equilibrium”, *the European Physical Journal D - Atomic, Molecular, Optical and Plasma Physics*, Vol. 11, Issue. 2, pp. 279–289, 2000.
12. Eisazadeh-Far, K., Metghalchi, H. and Keck, J. C., “Thermodynamic Properties of Ionized Gases at High Temperatures”, *Journal of Energy Resources Technology*, Vol. 133, Issue. 2, 022201, pp. 1-6, 2011.
13. Colonna, G., D’Angola, A. and Capitelli, M., “Electronic Excitation and Isentropic Coefficients of High Temperature Planetary Atmosphere Plasmas”, *Physics of Plasma*, Vol. 19, Issue. 7, 072115, pp. 1-9, 2012.
14. Baritello, V., Porcelli, F. and Subba, F., "Plasma-wall boundary layers", *Physical Review E*, Vol. 60, pp. 4733-4742, 1999.
15. Fay, J.A., “Plasma Boundary Layers”, United States Atomic Energy Comission, AD No. 294152, 1961.
16. American Society for Testing and Materials, “Standard Practice for Measuring Plasma Arc Gas Enthalpy by Energy Balance”, *ASTM Standard Designation: E 341-96*, 1996.

17. McBride, B.J., Zehe, M.J. and Gordon, S., "NASA Glenn Coefficients for Calculating Thermodynamic Properties of Individual Species", NASA TP-2002-211556, 2002.
18. McBride, B.J., Gordon, S. and Reno, M.A., "Thermodynamic Data for Fifty Reference Elements", NASA TP-3287/REV1, 2001.
19. Gordon, S. and McBride, B.J., "Thermodynamic Data to 20000 K for Monatomic Gases", NASA TP-1999-208523, 1999.
20. Svehla, R.A., "Transport Coefficients for the NASA Lewis Chemical Equilibrium Program", NASA TM-4647, 1995.
21. McBride, B. J., and Gordon, S., Computer "Program for Calculating and Fitting Thermodynamic Functions", *NASA RP-1271*, 1992.
22. Antsupov, A.V., "General Properties of Underexpanded and Overexpanded Supersonic Gas Jets", *Soviet Physics Technical Physics*, Vol. 19, No. 2, pp. 234-238, 1974.